Notes on Numerical Fluid Mechanics

The aim of this series is to publish promptly and in a detailed form new material from the field of Numerical Fluid Mechanics including the use of advanced computer systems. Published are reports on specialized conferences, workshops, research programs, and monographs.

This volume contains invited and contributed papers, presented at the Workshop on Large-Scale Scientific Computations held on June 7–11, 1997 in Varnar, Bulgaria.
The topics covered include high performance iterative methods and robust preconditioners, parallel methods for flow computations, adaptive sparse grids, multiscale methods, domain decomposition, preconditioners for parameter dependent and saddle-point problems, structured sparse matrices and numerical simulation of air pollution and contaminant transport.

Addresses of the editors of this volume:

Prof. Dr. *M. Griebel*, Institute of Appl. Math., University of Bonn, Wegelerstr. 6, D-53115 Bonn, Germany

Prof. Dr. *O. P. Ilie* , IMI-BAS, „Acad. G. Bontchev“, bl.8, Sofia, 1113 Bulgaria

Prof. Dr. *S. D. Margeno* and Prof. Dr. *P. S. Vassile ski*, CLPP-BAS, „Acad. G. Bontchev“, bl.25 A, Sofia, 1113 Bulgaria

ISSN 0179-9614
ISBN 3-528-06962-7

vieweg

UNESCO
Griebel/Iliev/Margenov/Vassilevski
Large-Scale Compution of Engineering and Environmental Problems
NNFM 62
vieweg

Notes on Numerical Fluid Mechanics

Volume 62

Large-Scale Scientific Computations of Engineering and Environmental Problems

Edited by
Michael Griebel
Oleg P. Iliev
Svetozar D. Margenov
Panayot S. Vassilevski

vieweg
UNESCO

Implicit Scheme for Navier-Stokes Equations in Primitive Variables via Vectorial Operator Splitting

C. I. Christov
National Institute of Meteorology and Hydrology
Bulgarian Academy of Sciences, 66 Tsarigradsko Chaussee blvd
Sofia 1784, Bulgaria

R. S. Marinova
Dept. of Mathematics, Technical University of Varna
1 Studentska str., Varna 9010, Bulgaria

Summary

The incompressible steady Navier-Stokes equations in primitive variables are coupled by the Poisson equation for pressure. Fictitious time is added and vectorial operator splitting is employed leaving the system coupled at each fractional-time step. Practical convergence and approximation of the scheme are verified. The lid-driven $2D$ flow in a rectangular cavity is considered as featuring example. Grids up to 513×513 are used and results are presented for Reynolds numbers as large as $Re = 10000$. They are in very good quantitative agreement with published data.

Key words: Navier-Stokes, Operator Splitting, Fractional steps.

1 Introduction

The Navier-Stokes equations are coupled through the nonlinear terms, the continuity equation and the boundary conditions. For internal flows the pressure is not prescribed on the boundaries. It can be eliminated from the equations by means of stream function and vorticity function ($\psi - \omega$ formulation in $2D$), but then boundary condition for vorticity is absent.

The implicit nature of pressure (vorticity function) requires special care for the stability of algorithms since the explicit decoupling of the boundary conditions (descendant of the so-called Thom's condition) imposes significant limitations on the time increment [18, 22, 5, 6, 12].

There exist in the literature different approaches to the problems of decoupling. The continuity equation is decoupled by the Chorin method of fractional steps (see [13]) in which the velocity field is predicted on the first half-time step and then the pressure is adjusted on the second half-time step so that the momentum equations are projected on divergence-free vector field. A comprehensive account of the progress recently made along these lines can be found in [15] where the $3D$ problem is also treated. This kind of methods are called "semi-explicit".

The boundary-condition problem has also received considerable attention. In $\psi - \omega$ formulation Ghia *et al.* [8] elaborated the iterative Thom's condition. Different algorithms for coupled solution of the $\psi - \omega$ equations were developed in [7, 16, 12] among many others. In primitive variables Vanka [23] uses an algorithm for coupled solving Navier-Stokes equations with central differences. See, e.g., [9] for a comprehensive review on this subject.

Vectorial version of the method of coordinate splitting of operator was proposed in [18] for $\psi - \omega$ formulation and a specialized solver was developed. Following the idea of coordinate splitting for bi-harmonic operators from [1] a fully implicit implementation of the boundary conditions is achieved in recent authors' works [5, 6] by means of a splitting scheme for the fourth-order stream-function equation (see, also [4, 3] for another applications of operator splitting for bi-harmonic operators).

If instead of the continuity equation one uses the Poisson equation for pressure one can add fictitious time and render the original system into a set of three coupled parabolic equations for u, v and p. One-to-one correspondence to the original system holds if the continuity equation is satisfied on the boundaries. This leads to overposed problem for the velocity components if decoupled from the pressure.

In the present paper a vectorial version of the operator-splitting implicit scheme is proposed which preserves the coupling between the sought functions at each fractional-time step allowing one to satisfy the boundary conditions without iterations. The approximation and stability of the scheme in full time steps is achieved after the continuity equation is added to the Poisson equation for the pressure and dully splitted.

In order not to obscure the main ideas of the method we consider only regions with rectilinear boundaries in cartesian coordinates. The grid is assumed uniform and staggered. For the nonlinear terms conservative approximation with central differences is used alleviating thus the problem of artificial viscosity. As a featuring example the lid-driven viscous incompressible flow in a rectangular cavity is treated.

2 Posing the problem

The $2D$ viscous incompressible flow is governed by the Navier-Stokes equations

$$\frac{1}{Re}\left(\frac{\partial^2 u}{\partial x^2}+\frac{\partial^2 u}{\partial y^2}\right)-\frac{\partial p}{\partial x}-\frac{\partial u^2}{\partial x}-\frac{\partial uv}{\partial y}=0, \tag{1}$$

$$\frac{1}{Re}\left(\frac{\partial^2 v}{\partial x^2}+\frac{\partial^2 v}{\partial y^2}\right)-\frac{\partial p}{\partial y}-\frac{\partial uv}{\partial x}-\frac{\partial v^2}{\partial y}=0, \tag{2}$$

coupled by the continuity equation

$$\frac{\partial u}{\partial x}+\frac{\partial v}{\partial y}=0, \tag{3}$$

where $u=u(x,y)$, $v=v(x,y)$ are the velocity components; $p=p(x,y)$ — the pressure. The Reynolds number is $Re=UL/\nu$, where U is the characteristic velocity, L — characteristic length, ν — kinematic coefficient of viscosity.

Upon applying the operation div to (1), (2) and acknowledging the continuity equation one obtains an explicit expression for p called "Poisson equation for pressure". However, for internal flows no boundary conditions are available for p and the very Navier-Stokes equations (1), (2) are to be taken on the respective boundary [11]. The formulation with Poisson equation for pressure is equivalent to the original system only if the continuity equation (3) is satisfied also on the boundaries.

The Poisson equation is multiplied by $1/Re$ and from the result the continuity equation (3) is subtracted (the latter is of crucial importance for the properties of the scheme). Thus

$$\frac{1}{Re}\left(\frac{\partial^2 p}{\partial x^2}+\frac{\partial^2 p}{\partial y^2}\right)-\frac{\partial u}{\partial x}-\frac{\partial v}{\partial y}+\frac{1}{Re}\left(\frac{\partial^2 u^2}{\partial x^2}+2\frac{\partial^2 uv}{\partial x\partial y}+\frac{\partial^2 v^2}{\partial y^2}\right)=0. \tag{4}$$

We add derivatives with respect to a fictitious time t and render the equations for u, v and p into the following vectorial system for $\vec{\theta}$:

$$\frac{\partial\vec{\theta}}{\partial t}=(\Lambda_1+\Lambda_2)\vec{\theta}+F[\vec{\theta}]. \tag{5}$$

where $\vec{\theta}=\mathrm{column}[u,v,p]$, $F[\vec{\theta}]=\mathrm{column}[0,0,F^p]$

$$\Lambda_1=\begin{pmatrix} L_{xx}-C_x & 0 & -L_x\\ 0 & L_{xx}-C_x & 0\\ -L_x & 0 & L_{xx}\end{pmatrix},\quad \Lambda_2=\begin{pmatrix} L_{yy}-C_y & 0 & 0\\ 0 & L_{yy}-C_y & -L_y\\ 0 & -L_y & L_{yy}\end{pmatrix},$$

$$F^p=\frac{1}{Re}\left(\frac{\partial^2 u^2}{\partial x^2}+2\frac{\partial^2 uv}{\partial x\partial y}+\frac{\partial^2 v^2}{\partial y^2}\right),$$

$$L_{xx}=\frac{1}{Re}\frac{\partial^2}{\partial x^2},\quad L_{yy}=\frac{1}{Re}\frac{\partial^2}{\partial y^2},\quad L_x=\frac{\partial}{\partial x},\quad L_y=\frac{\partial}{\partial y}.$$

Here C_x, C_y stand for the splitted nonlinear convective terms. For the sake of brevity only their difference approximations (9) are given explicitly in the present paper.

The flow in the lid-driven cavity occupies the region $\mathcal{D}=\{0\le x\le 1,\ 0\le y\le 1\}$ and the boundary conditions read

$$u(x,0)=u(0,y)=u(1,y)=0,\ u(x,1)=1;\ v(x,0)=v(x,1)=v(0,y)=v(1,y)=0.$$

with the additional conditions for the stemming from the continuity equation

$$\left.\frac{\partial u}{\partial x}\right|_{(0,y)}=\left.\frac{\partial u}{\partial x}\right|_{(1,y)}=0,\qquad \left.\frac{\partial v}{\partial y}\right|_{(x,0)}=\left.\frac{\partial v}{\partial y}\right|_{(x,1)}=0. \tag{6}$$

3 Difference scheme

We split the operator $\Lambda_1+\Lambda_2$ according to the scheme of stabilizing correction which is of first order in time, but has advantage for non-commuting operators (see [24]):

$$\frac{\vec{\theta}^{n+1/2}-\vec{\theta}^{n}}{\tau}=\Lambda_1\vec{\theta}^{n+1/2}+\Lambda_2\vec{\theta}^{n}+F[\vec{\theta}^{n}],\quad \frac{\vec{\theta}^{n+1}-\vec{\theta}^{n+1/2}}{\tau}=\Lambda_2(\vec{\theta}^{n+1}-\vec{\theta}^{n}). \tag{7}$$

Here τ is the increment of the fictitious time. Denote $I=\begin{pmatrix}E&0&0\\0&E&0\\0&0&E\end{pmatrix}$, where E is the unitary operator. The half-time-step variable $\vec{\theta}^{n+1/2}$ can be excluded to get

$$(I+\tau^2\Lambda_1\Lambda_2)\frac{\vec{\theta}^{n+1}-\vec{\theta}^{n}}{\tau}=(\Lambda_1+\Lambda_2)\vec{\theta}^{n+1}+F[\vec{\theta}^{n}]. \tag{8}$$

which is an implicit scheme of first-order of approximation $O(\tau)$. Due to the fact that the continuity equation has been added in the equation for pressure, the operator $I + \tau^2\Lambda_1\Lambda_2$ becomes a positive-definite on the divergence-free solutions when the iterations converge. Therefore the splitting scheme is stable when the calculations start close enough to the solution.

We employ uniform mesh in both directions. The mesh is staggered for u in direction x and for v in direction y (see Fig. 1-a) which is consistent with other works on (u, v, p) formulation. It allows one to use central differences for the boundary conditions on two-point stencils.

The number of grid lines in the two directions is N_x and N_y, respectively. The spacings are $h_x = 1/(N_x - 1)$, $h_y = 1/(N_y - 1)$ and $(x_i, y_j) = [(i-1)h_x, (j-1)h_y]$ for $i = 1, \dots, N_x$, $j = 1, \dots, N_y$.

In Fig. 1-b the pressure is sampled on the points labeled by '$\bullet$'; function u — in '$\circ$'; function v — in '$*$' and the notations $p_{i,j} = p(x_i, y_j)$, $u_{i,j} = u(x_i - \frac{1}{2}h_x, y_j)$, $v_{i,j} = v(x_i, y_j - \frac{1}{2}h_y)$ are used. We employ second-order conservative central-difference approximations for the operators in eq.(7), e.g., for C_x, C_y [14]:

$$
\begin{aligned}
C_x u_{i,j} &= \frac{(u^n_{i+1,j} + u^n_{i,j})u_{i+1,j} - (u^n_{i,j} + u^n_{i-1,j})u_{i-1,j}}{4h_x}, \\
C_y u_{i,j} &= \frac{(v^n_{i,j+1} + v^n_{i-1,j+1})u_{i,j+1} - (v^n_{i,j} + v^n_{i-1,j})u_{i,j-1}}{4h_y}, \\
C_x v_{i,j} &= \frac{(u^n_{i+1,j} + u^n_{i+1,j-1})v_{i+1,j} - (u^n_{i,j} + u^n_{i,j-1})v_{i-1,j}}{4h_x}, \\
C_y v_{i,j} &= \frac{(v^n_{i,j+1} + v^n_{i,j})v_{i,j+1} - (v^n_{i,j} + v^n_{i,j-1})v_{i,j-1}}{4h_y}.
\end{aligned}
\tag{9}
$$

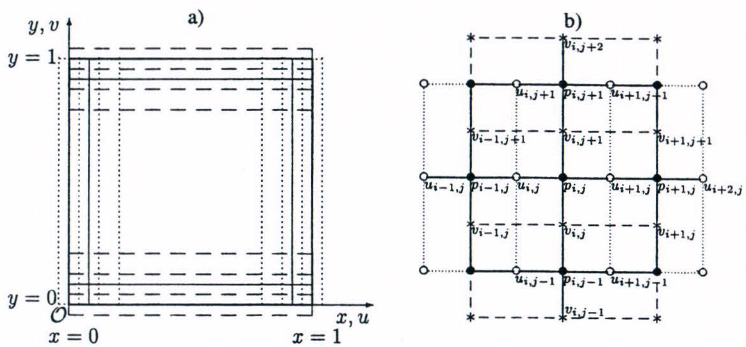

Figure 1: Computational domain, grid and finite-difference stencil.

Along the line $y = y_j$ one has to solve two linear algebraic systems: one for the set function $v^{n+\frac{1}{2}}_{i,j}$ with three-diagonal matrix, and another – for the vectorial set function $\mathbf{w}^{n+1/2} = \text{column}[u^{n+1/2}_{1,j}, p^{n+1/2}_{1,j}, \dots, u^{n+\frac{1}{2}}_{i,j}, p^{n+\frac{1}{2}}_{i,j}, \dots, u^{n+1/2}_{N_x,j}, p^{n+1/2}_{N_x,j}, u^{n+1/2}_{N_x+1,j}]$ with five-diagonal matrix.

In the same manner, the second half-time step along the line $x = x_i$ requires to solve a three-diagonal system for the set function $u^{n+1}_{i,j}$ and a five-diagonal system for the vectorial function $\mathbf{z}^{n+1} = \text{column}[v^{n+1}_{i,1}, p^{n+1}_{i,1}, \dots, v^{n+1}_{i,j}, p^{n+1}_{i,j}, \dots, v^{n+1}_{i,N_y}, p^{n+1}_{i,N_y}, v^{n+1}_{i,N_y+1}]$.

The multidiagonal systems are solved by means of a specialized solver [2] which is a generalization of what is called Thomas algorithm in the English-language literature or "progonka" in the Russian-language one.

The iterations are terminated when the following criterion is satisfied

$$
\max_{i,j}\left|\frac{u^{n+1}_{i,j} - u^n_{i,j}}{\tau}\right| \le \varepsilon, \quad \max_{i,j}\left|\frac{v^{n+1}_{i,j} - v^n_{i,j}}{\tau}\right| \le \varepsilon, \quad \max_{i,j}\left|\frac{p^{n+1}_{i,j} - p^n_{i,j}}{\tau}\right| \le \varepsilon,
$$

for sufficiently small tolerance, say $\varepsilon = 10^{-6}$. The rate of decrease of maximal change in u, v and p with iterations (the L_1 norm) is found to vary with Reynolds number Re, time-step τ and iteration number. Fig. 2 shows the observed rate of convergence for two different Reynolds numbers. The conservative nature of the scheme clearly shows up in these figures. After the iterative process approaches fairly close the solution, the decrease of L_1 norm becomes monotone.

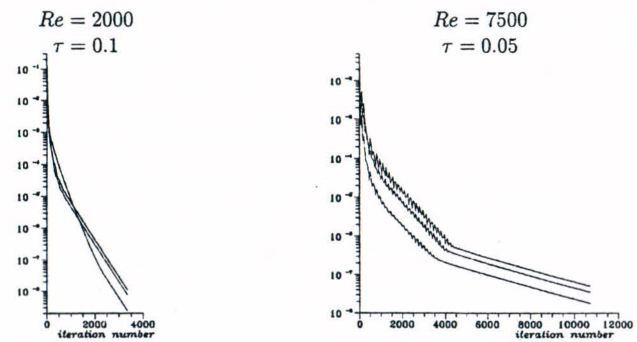

Figure 2: Rate of convergence $1/h = 512$, $\varepsilon = 10^{-6}$.

4 Tests and comparisons

To test the accuracy and efficiency of the scheme for $Re = 1000$ we obtain the solution on different grids: $h_x = h_y = h = 1/32, 1/64, 1/128, 1/256, 1/512$ and different time increments τ. The results confirm the full approximation of the scheme (no dependence on τ) and the $O(h^2)$ spatial approximation. Since we employ primitive variables the main characteristics to compare are the velocity components. The velocity profiles for u along the vertical cross section and v along the horizontal cross section trough the geometric center of the cavity are shown in Fig. 3 for several grid sizes. They are in close agreement between themselves as well as with the results of [8], the latter being widely accepted as a benchmark results.

More elaborate comparison of our results for the velocity profiles in the cross-sections through the geometric center of the cavity will be presented elsewhere.

5 Some further results for cavity flow

Driven cavity flow has always been a standard case study for any new scheme for Navier-Stokes equations. The advantage of this test problem is that its geometry is the simplest possible.

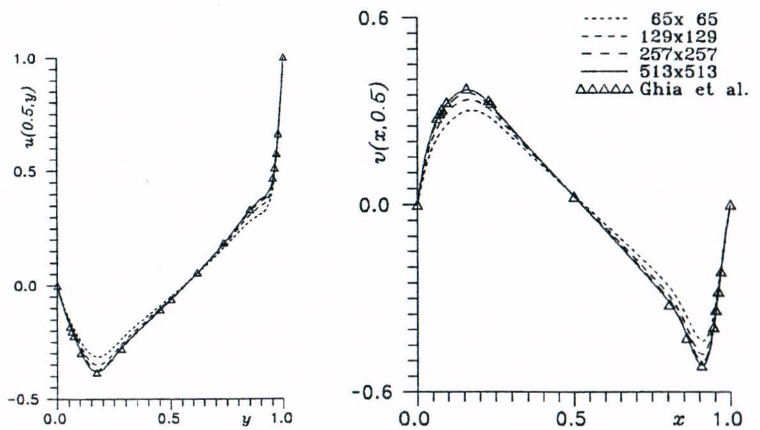

Figure 3: Velocity profiles through vortex center cavity, $Re = 1000$.

The disadvantage is that there are singularities in the points where the lid touches the vertical walls. It turns out, however, that the discontinuous boundary condition does not pose much difficulties. For moderately high Re, published results are available for this flow problem from a number of sources [5, 10, 13, 20, 23]. Some results are also available for high Re [17, 19], but the accuracy of many of these solutions has generally been regarded with certain skepticism because of the sizes of the computational meshes employed and of the difficulties with convergence. Exception to these may be the results obtained by Ghia *et al.* [8] and Turek [21] for $Re = 10000$ using multigrid and adaptive grid techniques for solution. Ghia *et al.* obtained highly accurate solutions using 257×257 grids. Schreiber and Keller [17] solved this problem using a sequence of grids of 180×180 points.

The streamline contours for different Re ranging from 1000 to 10000 are shown in Fig. 4 for grids of 513×513 nodes. They form a primary vortex the location of whose center as function of Reynolds number is shown in Fig. 5-a. The center of the primary vortex moves towards the geometric center of the cavity when Re increases.

Secondary vortices appear at the cavity corners. For smallest Re appears the vortex at the right-bottom corner. Its position as function of Reynolds number is shown in Fig. 5-b and compared to the literature data. The center of secondary vortex in the bottom right corner also moves towards the center with the increase of Re. Note that third-order accurate interpolation in the vicinity of centers of vortices is used to localize the position of local extrema of stream function.

For moderate Re a secondary vortex appears in the lower-left corner. The latest to appear is the secondary vortex at the top-left corner of the cavity. It is much more intricate in shape because of its close interaction with the discontinuity of the u component at the lid corner. To get an idea of how the shape of left-top secondary vortex depends on Re we conduct special set of calculations presented in Fig. 6.

Tertiary vortices appear in the lower-right corner of the cavity for $Re \approx 5000$ and in the lower-left corner for $Re \gtrapprox 7500$. These two tertiary vortices persist for different grids and are consistent with [8].

An interesting new observation of the present work is the appearance of a third tertiary

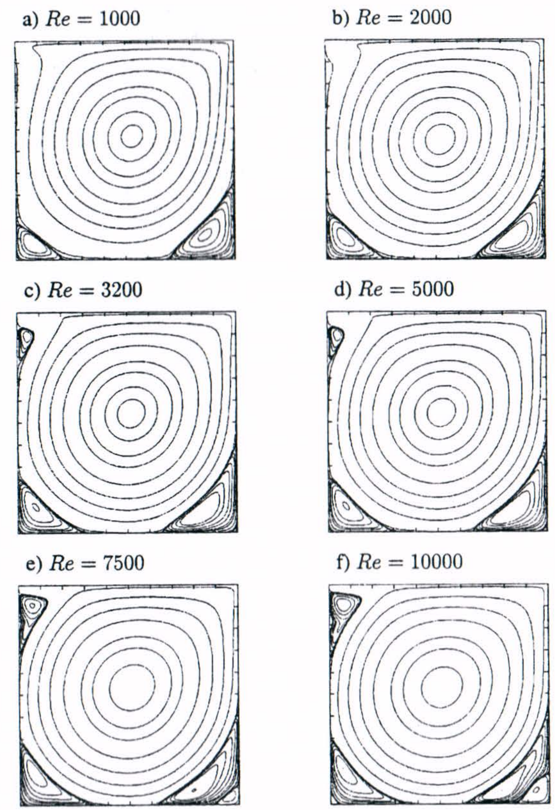

Figure 4: Streamline pattern. Contour values are: -0.115, -0.11, -0.10, -0.09, -0.07, -0.05, -0.03, -0.01, -1.0×10^{-4}, -1.0×10^{-5}, -1.0×10^{-7}, 0, 1.0×10^{-7}, 1.0×10^{-5}, 5.0×10^{-5}, 1.0×10^{-4}, 2.5×10^{-4}, 5.0×10^{-4}, 1.0×10^{-3}, 1.5×10^{-3}, 3.0×10^{-3}.

vortex in the top left corner of the cavity for $Re = 10000$. This tertiary vortex have not been observed in [8, 17, 19]. We believe it is very precious structure which heavily depends on the mesh size and on the approximations. All cited works from the literature employ upwind differencing which has smoothing effect regardless to the measure taken to achieve second order of approximation.

6 Conclusions

An efficient vectorial implicit operator-splitting method for steady Navier-Stokes equations is developed in which velocity and pressure are coupled on each fractional time step and the boundary conditions are resolved in fully implicit manner.

As a featuring example the lid-driven viscous incompressible flow in a rectangular cavity is treated by the new scheme. The mandatory numerical experiments are performed involving

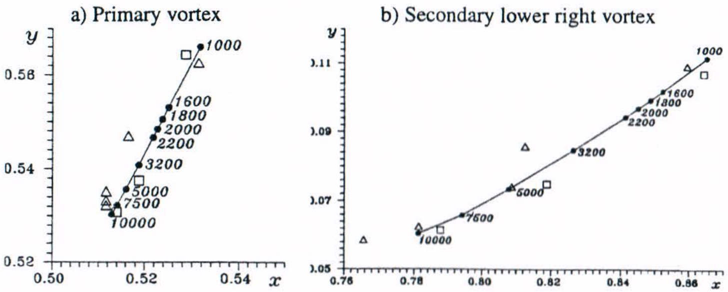

Figure 5: Effect of Re on location of vortex centers: $-\bullet-$: present results, $\triangle$: [8], $Re = 1000, 3200, 5000, 7500, 10000$, $\square$: [17], $Re = 1000, 4000, 10000$.

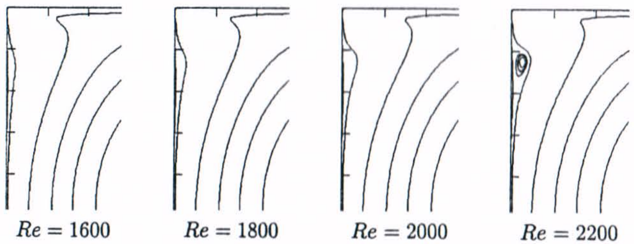

Figure 6: Secondary vortex at the left top corner.

different grids: 129×129; 257×257 and 513×513 points. The convergence of the scheme is verified. Stable calculations are conducted for Reynolds number up to $Re = 10000$. Results are in very good quantitative agreement with the known results from the literature.

Acknowledgment

Work supported in part by Grant MM-610/96 of National Science Foundation of Bulgaria.

References

[1] C. I. Christov, The method of variational imbedding for elliptic incorrect problems. *Comp. Rend. Acad. Bulg. Sci.*, **39**, No. 12, (1986), 23-26.

[2] C. I. Christov, Gaussian elimination with pivoting for multidiagonal systems. *University of Reading, Internal Report* **4**, 1994.

[3] C. I. Christov, and R. S. Marinova, Numerical Investigation of High Re Stationary Viscous Flow around Circular Cylinder as Inverse Problem, *Bulg. J. Meteorology & Hydrology*, **5**, No. 3–4 (1994), 105–118.

[4] C. I. Christov, J. Pontes, D. Walgraef, M. G. Velarde, Implicit time splitting for fourth-order Parabolic Equations, *Comp. Methods in Appl. Mech. Engn.* (1997), (to appear).

[5] C. I. Christov and A. Ridha, Splitting Scheme for Iterative Solution of Bi-Harmonic Equation. Application to $2D$ Navier-Stokes Problems. *Advances in Numerical Methods & Applications*, (I. T. Dimov et al., eds.), World Scientific (1994), 341–352.

[6] C. I. Christov and A. Ridha, Splitting Scheme for the stream-function formulation of $2D$ unsteady Navier-Stokes equations. *C. R. Acad. Sci. Paris*, **t. 320**, II b (1995), 441–446.

[7] B. Fornberg, A numerical study of steady viscous flow past a circular cylinder. *J. Fluid Mech.* **98** (1980), 819-835.

[8] U. Ghia, K. N. Ghia and C. N. Shin, High-Re solutions for incompressible flow using the Navier-Stokes equation and a multigrid method. *J. Comp. Phys.* **48** (1982), 387–411.

[9] Ph. M. Gresho, Incompressible fluid dynamics: Some fundamental formulation issues. *Ann. Rev. Fluid Mech.* **23** (1991), 413–453.

[10] Ph. M. Gresho and S. T. Chan, On the Theory of Semi-Implicit Projection Methods for Viscous Incompressible Flow and its Implementation via a Finite Element Method that also Introduces a Nearly Consistent Mass Matrix. Part 2: Implementation. *Int. J. Numer. Methods Fluids* **11**, (1990), 621–659.

[11] F. H. Harlow and J. E. Welch, Numerical Calculation of Time-Dependent Viscous Incompressible Flow of Fluid with Free Surfase. *Phys. Fluids*, **8**, No. 12 (1965), 2182–2189.

[12] O. P. Iliev and M. M. Makarov, A Block-Matrix Iterative Numerical Method for Coupled Solving $2D$ Navier-Stokes Equations. *J. Comp. Phys.*, **121** (1995), 324–330.

[13] J. Kim and P. Moin, Application of fractional-step method to incompressible Navier-Stokes equations. *J. Compt. Phys.* **59**, (1985), 308–323.

[14] G. I. Marchuk, *Methods of Computational Mathematics*, Nauka, Moskow, 1977.

[15] M. Rosenfeld, D. Kwak and M. Vinokur, A fractional step solution method for the unsteady incompressible Navier-Stokes equations in generalized coordinate system. *J. Comput. Phys.* **94** (1991), 102–137.

[16] S. G. Rubin and P. K. Khosla, Navier-Stokes calculations with a Coupled Strongly Implicit Method–I. *Computers and Fluids* **9** (1981), 163–180.

[17] R. Schreiber and H. B. Keller, Driven cavity flows by efficient numerical techniques. *J. Comput. Phys.* **49** (1983), 310–333.

[18] Sh. Smagulov and C. I. Christov, Iterationless numerical implementation of the boundary conditions in the vorticity-stream function formulation of Navier-Stokes equations. Preprint 20 *Inst. Theor. Appl. Mech.*, Russian Acad. Sci., Novosibirsk, (1980).

[19] J. Shen, Hopf Bifurcation of the Unsteady Regularized Driven Cavity Flow. *J. Comp. Phys.* (1991), 228–245.

[20] M. C. Thompson and J. H. Ferziger, An adaptive multigrid technique for the incompressible Navier-Stokes equations. *J. Comput. Phys.* **82** (1989), 94–121.

[21] S. Turek, Tools for simulating non-stationary incompressible flow via discretely divergence-free finite element models. *Int. J. Numer. Meth. Fluids*, **18** (1994), 71–105.

[22] P. N. Vabishchevich, Implicit finite-difference schemes for the nonstationary Navier-Stokes equations with the stream function and the vorticity as variables. *Differential equations*, **20** (1984), 820–827; translation from Differ. Uravn. **20**, No.7 (1984), 1135–1144.

[23] S. P. Vanka, Block-implicit multigrid solution of Navier-Stokes equations in primitive variables. *J. Comput. Phys.* **65** (1986), 138–158.

[24] N. N. Yanenko, Method of Fractional Steps, *Gordon and Breach*, 1971.